

Size separation of carbon nanotubes for biomedical applications

Yoshinori Sato^a, Yuki Akimoto^a, Balachandran Jeyadevan^a, Kenichi Motomiya^b,
Rikizo Hatakeyama^b, Kazuchika Tamura^c, Tsukasa Akasaka^c, Motohiro Uo^c, Atsuro Yokoyama^c,
Ken-ichiro Shibata^c, Fumio Watari^c, Kazuyuki Tohji*^a

^aGraduate School of Environmental Studies, Tohoku University, Sendai, 980-8579, Japan

^bGraduate School of Engineering, Tohoku University, Sendai, 980-8579, Japan

^cGraduate School of Dental Medicine, Hokkaido University, Sapporo, 060-8586, Japan

ABSTRACT

In this paper, we report the results of an attempt to disperse MWCNTs in water and determine their biocompatibilities. The length of the MWCNTs was reduced by treating the acidic nanotube suspension with ultrasonic irradiation. Then, the cut nanotubes were size-separated into 670, 550 and 220 nm length by filtration using polycarbonate membrane filters. The neutrophils activity (TNF- α) of size-separated MWCNTs was low and confirmed biocompatible.

Keywords: Multi-walled carbon nanotubes (MWCNTs), size separation, biocompatibility, neutrophils activity, TNF- α

1. INTRODUCCION

One of the challenging and exciting research areas is currently related to the bioactivity of carbon nanomaterials and their derivatives that have nano-spaces and large surface areas. Recently, carbon nanotubes (CNTs)¹⁻³ have been proposed for biomedical applications^{4,9}. However, water-solubilization of the CNTs is indispensable for biomedical fields. Since the CNTs have chemical properties similar to graphite and are several micrometers long, they do not easily disperse in water on their own. Though the solubilization can be improved with the use of surfactants, it may affect the intracellular reactions and also complex reaction-phenomena on the physiological cells and tissues¹⁰. Thus, techniques to make aqueous dispersions of CNTs without the use of surfactants are desirable. Also, prior to the application of these dispersions in biomedical fields, the assessment of the potential health hazard of water-soluble CNTs for humans is important¹¹⁻¹⁵. Here, we report the findings of a study carried out to disperse multi-walled carbon nanotubes (MWCNTs) in water by reducing the length of purified nanotubes by ultrasonically treating the tubes in an acidic medium, size-separate by the membrane filtration and their biocompatibilities by *in vitro* using human neutrophils of tumor necrosis factor-alpha (TNF- α).

2. EXPERIMENTAL DETAILS

2.1 Preparation of the size-separated MWCNTs

Purification procedure of MWCNTs. The MWCNTs synthesized by the CVD method and supplied by NanoLab was used in this study. The purity is 80 wt % with impurities such as amorphous carbon, Fe, Mo, Cr, Ni, and Al. The diameter is 20 – 40 nm, and the length is 5.0 μ m on the average. First, MWCNTs were burned at 773 K for 90 min under atmospheric pressure. Then, the burned product was transferred into a flask with 1.0 L of 6M-HCl and treated at 333 K for 12 hours to remove the metals or metal oxides. Following this, the acid solution was filtered using a PTFE membrane filter with 0.1 μ m pore size. The filtered cake was transferred into a flask with 1.0 L of 3M-NaOH and refluxed at 373 K for 15 hours to dissolve Aluminum oxides. The nanotubes are then recovered by filtering the suspension by using a membrane filter with 0.1 μ m pore size, and the filtered cake was rinsed out with hot water. Finally, the sample was dried up at 333 K for 12 hours.

Cutting procedure of the purified MWCNTs. The cutting procedure of the purified MWCNTs is as follows: 100 mg of the purified MWCNTs was suspended in 100 mL of a 3:1 (v/v%) mixture of concentrated H₂SO₄ (95%) / HNO₃ (60%) and exposed to ultrasonic irradiation for 5 hours¹⁶. The acid-treated MWCNTs were filtered using a membrane filter with a pore size of 0.1 μ m, and the filtered cake was rinsed out with water until the pH of filtrate becomes neutral.

Size separation procedure of the cut MWCNTs. The size separation procedure of the cut MWCNTs is as follows¹⁷: 20 mg of the cut MWCNTs was suspended in 400 mL of ethanol and irradiated by ultrasonic for 1 hour. Next, the suspension was centrifuged at 5000 g for 1 hour in order to remove the aggregation of a few microns long MWCNTs and then the supernatant was filtrated using polycarbonbonate membranes with cylindrical pore diameters 1.2, 0.8, and 0.4 μm .

Characterization of the purified and cut MWCNTs. The purified and cut MWCNTs were characterized with scanning electron microscope (SEM), transmission electron microscope (TEM), X-ray fluorescence spectroscopy (XRF), and Fourier transform infrared spectroscopy (FT-IR).

2.2 Biocompatibility test of the size-separated MWCNTs

Size-separated MWCNTs. Highly pure size-separated MWCNTs of 670, 550 and 220 nm were mixed with HBSS (Hanks' balanced salt solution) in concentrations of 0.5 $\mu\text{g}/\text{ml}$.

Cells used for toxicity test. Human peripheral blood was obtained from healthy volunteers in our group. Neutrophils were separated from blood using 6% isotonic sodium chloride containing hydroxyethyl starch and lymphocyte isolation solution. After the suspended size-separated MWCNTs solution was kept at 310 K for 2 weeks, neutrophils were added and incubated at 310 K for 30 min.

Cytokines (TNF- α). Tumor necrosis factor-alpha (TNF- α) production per 10^6 neutrophils in the supernatant was measured using ELISA kits.

3. RESULTS AND DISCUSSION

Figure 1 shows the SEM images of the raw (a), the purified MWCNTs (b) and the HRTEM image of the purified

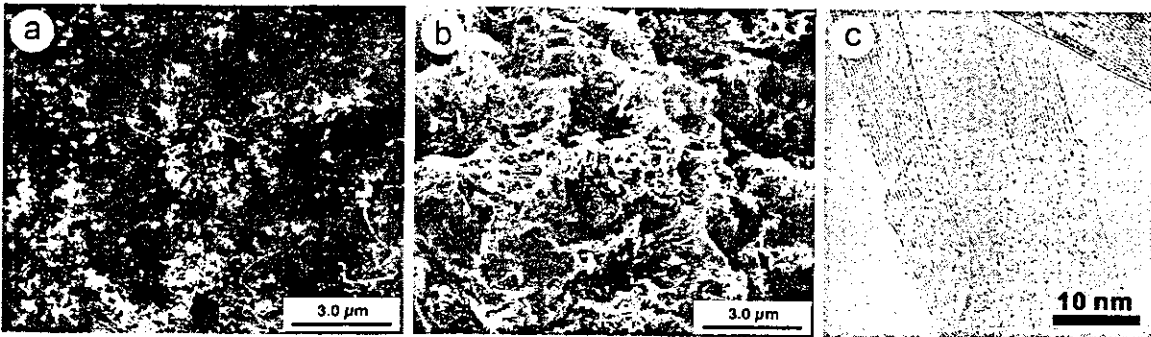


Figure 1. SEM images of the raw MWCNTs (a) and the purified MWCNTs (b). High magnification TEM image of the purified MWCNTs (c).

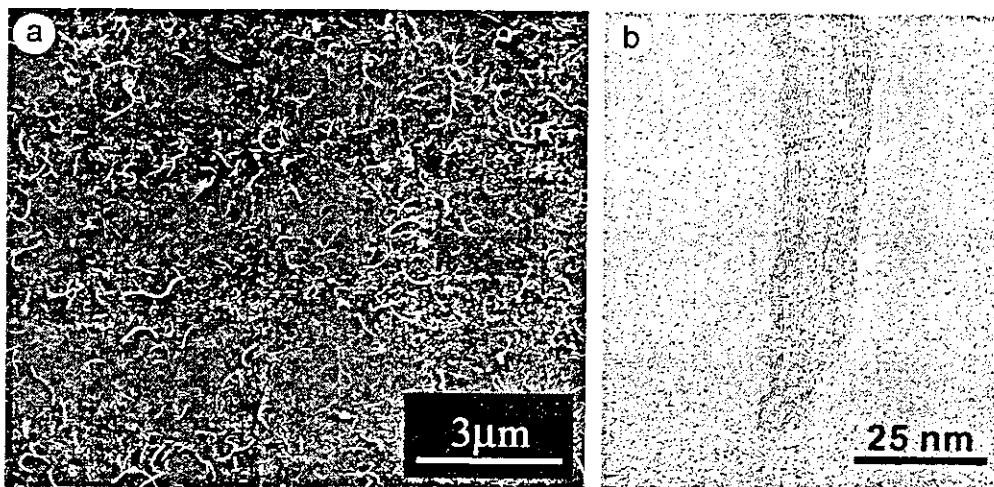


Figure 2. SEM and TEM images of the cut MWCNTs treated by the strong acids.

MWCNTs (c). It is clear from the SEM images that the purified MWCNTs were totally free of amorphous carbon and carbon nanoparticles. The purified MWCNTs were confirmed to be free of metal impurities from TEM-EDX and XRF analyses. Furthermore, clear (002) lattice image of the purified MWCNTs (Figure 1c) suggested their highly crystalline nature. However, these tubes consist of many bamboo-like structures¹⁸, and the diameter and length are not uniform in size.

Figure 2 shows the SEM (a) and TEM (b) images of the cut MWCNTs treated by the strong acids. It is obvious from the SEM image (Figure 2a) that the MWCNTs have been shortened and there is a large population of nanotubes that are less than 1.0 μm long. The cut nanotubes dispersed easily in the polar solvents such as ethanol and water. This may have become possible due to the reduced length and surface modification by the hydrophilic groups of the nanotube. However, the strong acid damaged the outer wall of MWCNTs, and the carbon network of MWCNTs was broken. However, the inner walls are intact. We believe that the property of the MWCNTs is retained.

We measured the FT-IR spectra of the cut MWCNTs in order to confirm the presence of the carboxyl and the hydroxyl groups (Figure 3). The IR spectrum of the cut MWCNTs has several peaks. The band between 1000 and 1200 cm^{-1} corresponds to stretching vibration of C-O and deformation vibration of OH. These bands are characterized by a shift to lower wavenumbers when a dimmer carboxyl is formed by hydrogen bonding¹⁹. The stretching vibration of aromatic C=C is observed between 1500 and 1600 cm^{-1} . On the other hand, the band between 2700 and 2900 cm^{-1} corresponds to the stretching vibration of CH attached to graphene edge. Also, the band around 3450 cm^{-1} is characteristic of the stretching vibration of OH and water. Thus, the surface of cut MWCNTs are modified by the carboxyl and hydroxyl functional groups and has made the dispersion of the same in water possible.

Figure 4 shows the SEM images (left) and their corresponding size-distribution (right) of the size-separated MWCNTs. The length of the nanotube becomes small, as the pore diameter of membrane filter is gradually decreased (Figure 4). The yield of MWCNTs with the average length of 220 nm (Figure 4c) was high compared with 670 and 550 nm (Figure 4a,b) length MWCNTs. These results demonstrate that we have been successful in isolating the cut nanotubes with average lengths 670, 550 and 220 nm. The IR analysis of the size-separated nanotube suggested that the surface structure depends on the length.

Figure 5 shows the amount of TNF- α released from neutrophils in HBSS containing size-separated nanotubes. For comparison, the amount of TNF- α released from neutrophils in HBSS containing Ti particles is plotted in the same graph²⁰. In the case of Ti particles, TNF- α is released for particles with diameter less than 2.0 μm . Concerning the

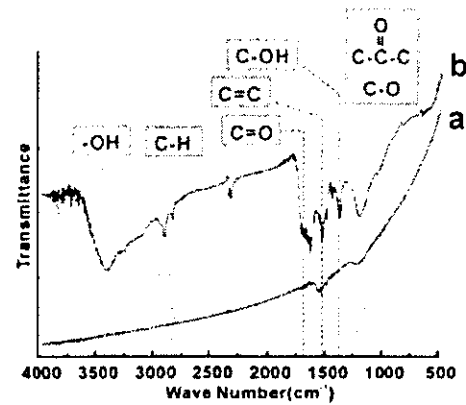


Figure 3. IR spectra of the purified MWCNTs (a) and the cut MWCNTs (b).

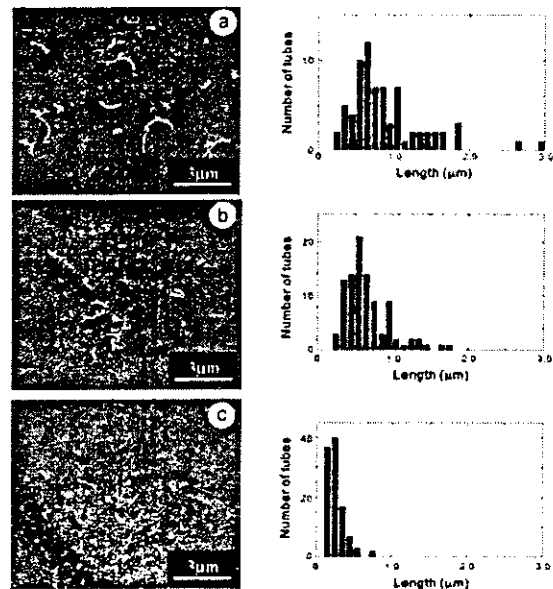


Figure 4. SEM images (left, a, b, c) and size-distribution (right) of the size-separated MWCNTs.

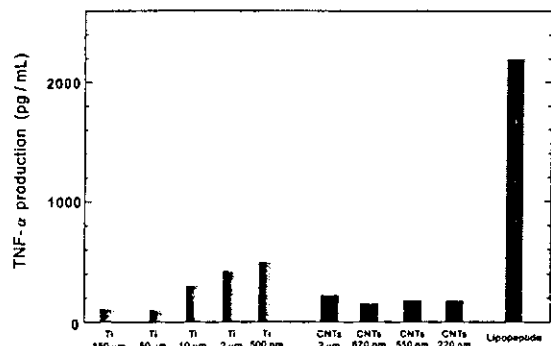


Figure 5. The amount of TNF- α released from neutrophils in HBSS containing size-separated nanotube and Ti particles.

relationship between cell and particle size on cytotoxicity, this effect is pronounced and the neutrophils activity increased²⁰ when the particles are smaller than the cell size. On the other hand, neutrophils activity is very low and their intensity does not depend on their size in the case of size-separated nanotubes shorter than 1.0 μm . Thus from our study, we could conclude that the carbon nanotubes are highly biocompatible. However, additional tests should be carried out to confirm the same.

4. CONCLUSION

We have succeeded in preparing highly pure size-separated MWCNTs. The biocompatibility test based on the neutrophils activity was carried out on these size-separated MWCNTs and proven to be non-toxic. The results of this study could be used to develop carbon-based materials for biomedical applications.

ACKNOWLEDGMENTS

This work was supported by Grant-in-Aid for Basic Research #(S) 14103016, and #(S) 13852016 from the Ministry of Education, Science, Culture and Sport of Japan and #H14-nano-021 from the Ministry of Health, Labor and Welfare.

REFERENCES

1. S. Iijima, "Helical Microtubules of Graphitic Carbon", *Nature*, **354**, 56-58, 1991.
2. S. Iijima and T. Ichihashi, "Single-Shell Carbon Nanotubes of 1-nm Diameter", *Nature* **363**, 603-605, 1993.
3. D. S. Bethune, C. H. Kiang, M. S. de Vries, G. Gorman, R. Savoy, J. Vazquez and R. Beyers, "Cobalt-Catalyzed Growth of Carbon Nanotubes with Single-Atomic-Layerwalls", *Nature* **363**, 605-607, 1993.
4. F. Belavoine, P. Schultz, C. Richard, V. Mallouh, T. W. Ebbesen and C. Mioskowski, "Helical Crystallization of Proteins on Carbon Nanotubes: A First Step toward the Development of New Biosensors", *Angew. Chem. Int. Ed.*, **38**, 1912-1915, 1999.
5. M. P. Mattson, R. C. Haddon and A. M. Rao, "Molecular Functionalization of Carbon Nanotubes and Use as Substrates for Neuronal Growth", *J. Mol. Neurosci.*, **14**, 175-182, 2000.
6. P. R. Supronowicz, P. M. Ajayan, K. R. Ullmann, B. P. Arulanandam, D. W. Metzger and R. Bisios, "Novel current-conducting composite substrates for exposing osteoblasts to alternating current stimulation", *J. Biomed. Mater. Res.*, **59**, 499-506, 2002.
7. A. Bianco and M. Prato, "Can Carbonnanotubes Be Considered Useful Tools for Biological Applications?", *Adv. Mater.*, **15**, 1765-1768, 2003.
8. D. Pantarotto, J. -P. Briand, M. Prato and A. Bianco, "Translocation of Bioactive Peptides across Cell Membranes by Carbon Nanotubes", *Chem. Comm.*, 16-17, 2004.
9. H. Hu, Y. Ni, V. Montana, R. C. Haddon and V. Parpura, "Chemically Functionalized Carbon Nanotubes as Substrates for Neuronal Growth", *Nano. Lett.*, **4**, 507-511, 2004.
10. R. Bandyopadhyaya, E. Nativ-Roth, O. Regev and R. Yerushalmi-Rozen, "Stabilization of Individual Carbon Nanotubes in Aqueous Solutions", *Nano Lett.*, **2**, 25-28, 2002.
11. V. L. Colvin, "The Potential Environmental impact of Engineered Nanomaterials", *Nat. Biotechnol.*, **21**, 1166-1170, 2003.
12. D. B. Warheit, B. R. Laurence, K. L. Reed, D. H. Roach, G. A. M. Reynolds and T. R. Webb, "Comparative Pulmonary Toxicity Assessment of Single-Wall Carbon Nanotubes in Rats", *Toxicol. Sci.*, **77**, 117-125, 2004.
13. C. -W. Lam, J. T. James, R. McCluskey and R. L. Hunter, D. B. Warheit, B. R. Laurence, K. L. Reed, D. H. Roach, G. A. M. Reynolds and T. R. Webb, "Comparative Pulmonary Toxicity Assessment of Single-Wall Carbon Nanotubes in Rats", "Pulmonary Toxicity of Single-Wall Carbon Nanotubes in Mice 7 and 90 Days after Intratracheal Instillation", *Toxicol. Sci.*, **77**, 126-134, 2004.
14. P. H. M. Hoet, A. Nemmar and B. Nemery, "Health Impact of Nanomaterials?", *Nat. Biotechnol.*, **22**, 19, 2004.
15. R. F. Service, "Nanomaterials Show Signs of Toxicity", *Science*, **300**, 243, 2003.
16. J. Liu, A. G. Rinzler, H. Dai, J. H. Hafner, R. K. Bradley, P. J. Boul, A. Lu, T. Iverson, K. Shelimov, C. B. Huffman, F. Rodriguez-Macias, Y. -S. Shon, T. R. Lee, D. T. Colbert and R. E. Smalley, "Fullerene Pipes", *Science*, **280**, 1253-1256, 1998.

17. T. Abatemarco, J. Stickel, J. Belfort, B. P. Frank, P. M. Ajayan and G. Belfort, "Fractionation of Multiwalled Carbon Nanotubes by Cascade Membrane Microfiltration", *J. Phys. Chem.*, **103**, 3534-3538, 1999.
18. C. J. Lee, J. H. Park and J. Park, "Synthesis of Bamboo-shaped Multiwalled Carbon Nanotubes using Thermal Chemical Vapor Deposition", *Chem. Phys. Lett.*, **323**, 560-565, 2000.
19. H. -U. Gremlich and B. Yan, *Infrared and Raman Spectroscopy of Biological Materials*, Marcel Dekker, New York, 2002.
20. K. Tamura, N. Takashi, R. Kumazawa, F. Watari and Y. Totsuka, "Effects of Particle Size on Cell Function and Morphology in Titanium and Nickel", *Mater. Trans.*, **43**, 3052-3057, 2002.

*tohji@mail.kankyo.tohoku.ac.jp; phone +81 22 217 7390; fax +81 22 217 7390

Biocompatibility of carbon nanotube disk

Yoshinori Sato^{*a}, Makoto Ohtsubo^a, Balachandran Jeyadevan^a, Kazuyuki Tohji^a, Kenichi Motomiya^b, Rikizo Hatakeyama^b, Go Yamamoto^c, Mamoru Omori^c, Toshiyuki Hashida^c, Kazuchika Tamura^d, Tsukasa Akasaka^d, Motohiro Uo^d, Atsuro Yokoyama^d, Fumio Watari^d

^aGraduate School of Environmental Studies, Tohoku University, Sendai, 980-8579, Japan

^bGraduate School of Engineering, Tohoku University, Sendai, 980-8579, Japan

^cFracture and Reliability Research Institute, Tohoku University, Sendai, 980-8579, Japan

^dGraduate School of Dental Medicine, Hokkaido University, Sapporo, 060-8586, Japan

ABSTRACT

We report the preparation, properties and biocompatibility of multi-walled carbon nanotube (MWCNT) disk. Sintered Multi-walled carbon nanotube disk was fabricated by spark plasma sintering the MWCNT and phenol resin mixture by using the Spark Plasma System (SPS) under 1273 K and 80 MPa in vacuum. As the concentration of phenol resin in the sintered MWCNT disk increases, the bending strength and Young's modulus increased. However, the inflammatory response was observed in the tissue exposed to the surface of the sintered MWCNT disk. This was believed due to the residual phenol resin in the disk. The result indicates that the disk has to be annealed at higher temperatures under inert gas atmosphere to perfectly convert phenol resin to graphitic materials.

Keywords: Multi-walled carbon nanotubes (MWCNTs), spark plasma system (SPS), inflammatory response, biocompatibility, fibrous connective tissue, lymphocyte

1. INTRODUCCION

Carbon composites have been proposed as an alternate biomaterial for dental and internal organ that require high bending strength with lightweight. Until now, C/C (carbon-carbon) composites have been considered for artificial heart valves^{1,2} and tooth roots³. However, the mechanical strength has not been high enough. On the other hand, carbon nanotubes (CNTs)⁴⁻⁶ and their composites⁷⁻¹⁰ and fibers¹¹⁻¹⁶ have been proposed to be used in the field of aerospace technology because the CNTs have unique mechanical properties such as 0.3-1.0 TPa of high Young's modulus and 11-200 GPa of tensile strength¹⁷. We believe that the carbon nanotubes have potential to replace the traditional biomaterials. Here, we report the preparation, mechanical properties and biocompatibility of the sintered multi-walled carbon nanotube disk.

2. EXPERIMENTAL DETAILS

2.1 Materials and characterization

Purification of MWCNTs. We used the MWCNTs synthesized by the CVD method (NanoLab Inc., US, 80 wt% purity). The impurities were amorphous carbon, Fe, Mo, Cr, Ni, and Al. The diameter lies between 20 and 40 nm, and the average length is 5.0 μm . First, MWCNTs were burned at 773 K for 90 min under atmospheric pressure. The burned product was then transferred into a flask with 1.0 L of 6M-HCl and treated at 333 K for 12 hours to remove the metals or metal oxides except aluminum oxide. Following this, the suspension was filtered using a PTFE membrane with the pore size of 0.1 μm . The filtered cake was transferred into a flask with 1.0 L of 2M-NaOH and refluxed at 373 K for 15 hours to dissolve aluminum oxides. The suspension was then filtered using a membrane filter (PTFE membrane with the pore size of 0.1 μm) and the filtered cake was washed. Finally, the sample was dried at 333 K for 12 hours. The structure of the sintered MWCNT disk was

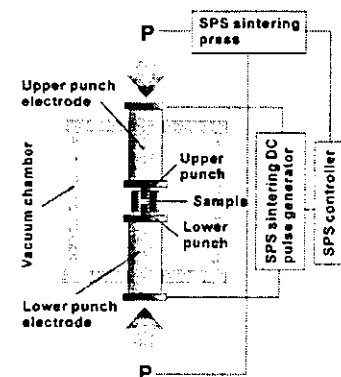


Figure 1. Illustration of Spark Plasma System (SPS).

characterized with scanning electron microscope (SEM), transmission electron microscope (TEM), X-ray fluorescence spectroscopy (XRF), and Fourier transform infrared spectroscopy (FT-IR).

Preparation of MWCNT disk. Sintered Multi-walled carbon nanotube disk was fabricated by spark plasma sintering the MWCNT and phenol resin mix by using the spark plasma system (SPS) under 1273 K and 80 MPa in vacuum for 1 hour. The SPS has been developed for sintering of metal and ceramics in the plasma and electric field, and it is used for consolidation of various kinds of materials such as metals, ceramics and polymer^{18,19}. This system consists of vacuum chamber, punch electrodes, graphite die, SPS DC-pulse power generator, SPS sintering press, and SPS controller (Figure 1). The nanotube powders were put in a graphite die with 10 mm diameter hole and set in the SPS. The mechanical property of the MWCNT disk was measured by using a small punch test (SP). The SP equipment consists of the puncher, upper and lower die. The specimen (MWCNT disk) is subjected to a puncher driven at a constant displacement rate through the guide hole, and the puncher force and displacement were recorded.

2.2 Biocompatibility test of the sintered MWCNT disk

A rectangular parallelepiped MWCNT of 1.5 x 1.5 x 5.0 mm in size was used as an implant material. The sample was implanted in the subcutaneous connective tissue in the abdominal region of Wistar strain rats. After the rats were anesthetized with diethyl ether, pentobarbital sodium was injected into the abdominal cavity of the rats and the metal implants were inserted in the subcutaneous connective tissue in the abdominal region of the rats to observe the response of soft tissue. After one week, the MWCNT disk implanted in the subcutaneous tissue was carefully removed from the resected tissue block after fixation in 10% neutral buffered formalin, and the tissue block was embedded in paraffin by the conventional method. The tissue block was sectioned and stained with hematoxylin-eosin^{20,21}. These specimens were observed with an optical microscope. When inflammatory response arises, fibrous connective tissue becomes thick and lymphocyte is observed in the fibrous connective tissue.

3. RESULTS AND DISCUSSION

Figure 2a shows the SEM image of the purified MWCNTs. It is clear that the purified MWCNTs were totally free of amorphous carbon and carbon nanoparticles. These tubes consist of many bamboo-like structures (Figure 2b), and the diameter and length are not uniform in size. The phenol resin and the purified MWCNTs were dispersed into ethanol and sonicated for 1 hour. The amount of phenol resin in the MWCNT-phenol resin mixture was fixed at 25 and 50 wt%. Next, the ethanol was evaporated at 343 K under atmospheric pressure, and the mixtures were heated at 573 K for 1 hour under N₂ atmosphere to convert the phenol resin into carbon materials.

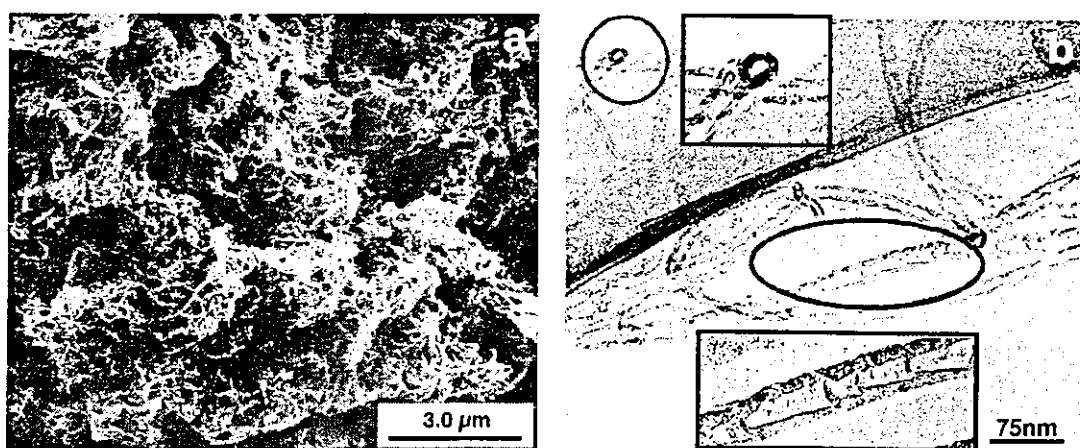


Figure 2. SEM image of the purified MWCNTs (a) and TEM image of the MWCNTs with bamboo-like structure (b).

Figure 3 shows the SEM image of MWCNTs in the MWCNT-phenol resin mixture with 50 wt% phenol resin. The arrows in Figure 3 indicate the areas of decomposed phenol resins. Figure 4 is the photograph of the sintered MWCNT disk with 10 mm in diameter and 1.5 mm in thick. The MWCNT disk that could withstand the mechanical test (SP) was prepared successfully. Table 1 shows the bending strength, Young's modulus and apparent density of the

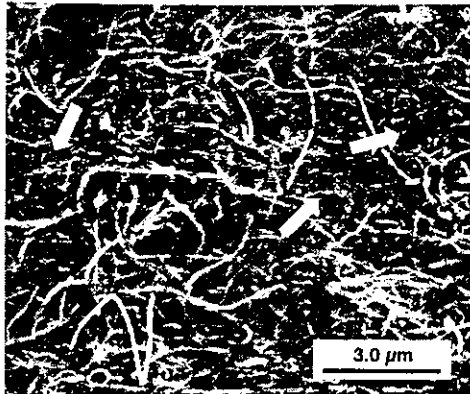


Figure 3. SEM image of MWCNTs with 50 wt% phenol resin. Arrows are the decomposed phenol resins.

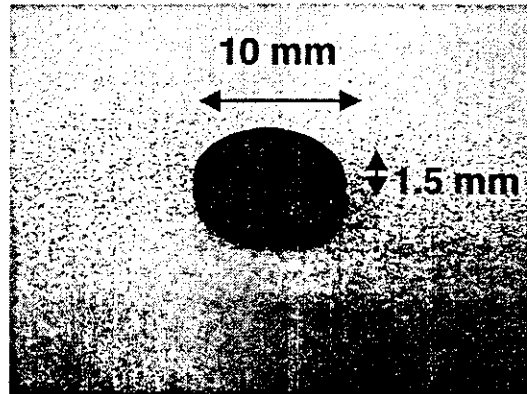


Figure 4. The photograph of the sintered MWCNTs disk produced by SPS.

sintered MWCNT disk. The mechanical properties determined from the SP test of the MWCNT disk prepared with 25 wt% phenol resin, were 72.7 MPa (bending strength), 1.5 GPa (Young's modulus), and 1.38 g/cm³ (apparent density). On the other hand, the mechanical properties of the MWCNT disk prepared with 50 wt% phenol resin were determined to be 91.4 MPa (bending strength), 2.3 GPa (Young's modulus), and 1.41 g/cm³ (apparent density). Our results clearly indicate that the mechanical strength is improved when the amount of phenol resin in the MWCNT-phenol resin mixture was increased. However, the recorded mechanical properties were not high enough in comparison with the human bone². The reason for the low value can be either due to weak bonding between tubes or binder and the tube

Table 1. Mechanical properties and apparent density of the sintered MWCNT disk.

Material	Bending strength (MPa)	Young's modulus (GPa)	Apparent density (g/cm ³)
MWCNTs disk with 25 wt%	72.2	1.53	1.38
MWCNTs disk with 50 wt%	91.4	2.36	1.41
Human bone	150	16-18	—

Figure 5 shows the optical micrographs of the tissue response to the sintered MWCNT disk with 50 wt. % phenol resin in the subcutaneous tissue of rat after one week. Figure 5b is the higher magnification optical micrograph of the rectangle frame shown in the figure 5a. The sintered MWCNT disk implants were encapsulated with thick fibrous connective tissue, with some lymphocytes (circled in Figure 5b). This tendency was also observed in the sintered MWCNT disk with 25 wt % phenol resin. These results are an indication of inflammatory response. On the other hand, in case of the C/C composite implants, the fibrous connective tissue is thin and no inflammatory response was observed. Thus, the sintered MWCNT disk prepared with phenol resin as binder is believed to be less biocompatible. One of the reasons for the inflammatory response is due to the residue of undecomposed phenol resin in the sintered MWCNT disk.

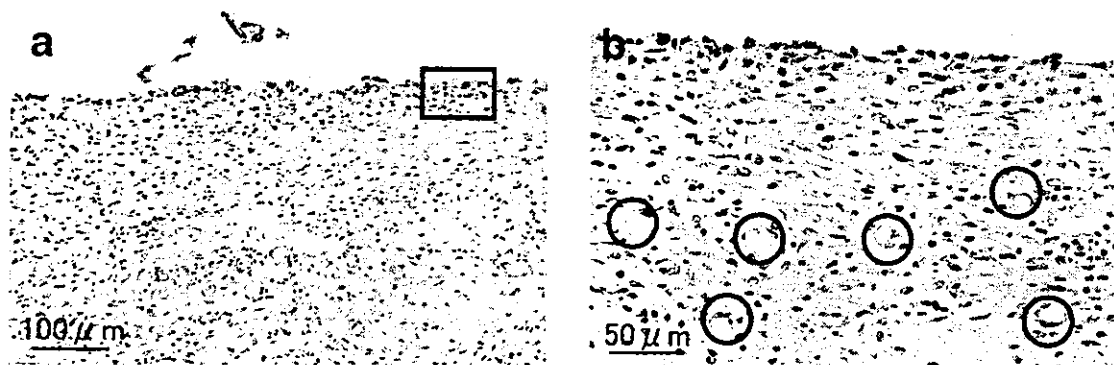


Figure 5. Optical micrographs of the tissue response to the sintered MWCNT disk mixed with 50 wt% in the subcutaneous tissue of rat after one week. Figure 5b is the high magnification optical micrograph of a squire frame in the Figure 5a. Lymphocytes are in open circles.

4. CONCLUSION

Sintered multi-walled carbon nanotube disk was produced by SPS under the condition of 1273 K at 80 MPa in vacuum. As the concentration of the phenol resin is increased in the sintered MWCNT disk, the bending strength and Young's modulus increased. However, the recorded mechanical properties were not high enough to consider it as an alternative to human bone. Though the mechanical properties were improved with higher phenol resin concentration, the inflammatory response was observed in the tissue exposed to the surface of the sintered MWCNT disk. The inflammatory response is the residue of undecomposed phenol resin in the sintered MWCNT disk. In order to improve the biocompatibility of sintered MWCNT disk, the disk has to be annealed at higher temperatures under inert gas atmosphere to totally convert phenol resin to graphite.

ACKNOWLEDGMENTS

This work was supported by Grant-in-Aid for Basic Research #(S) 14103016, and #(S) 13852016 from the Ministry of Education, Science, Culture and Sport of Japan and #H14-nano-021 from the Ministry of Health, Labor and Welfare.

REFERENCES

1. J. C. Bokros, "Carbon Biomedical Devices", *Carbon*, **15**, 353-371, 1977.
2. A. D. Haubold, H. S. Shim, J. C. Bokros, "Developments in Carbon Prosthetics", *Biomaterials Medical Devices and Artificial Organs*, **7**, 263-269, 1979.
3. G. M. Jenkins, "Biomedical Applications of Carbon-Fiber Reinforced Carbon in Implanted Prostheses", *Carbon*, **15**, 33-37, 1977.
4. S. Iijima, "Helical Microtubules of Graphitic Carbon", *Nature*, **354**, 56-58, 1991.
5. S. Iijima and T. Ichihashi, "Single-Shell Carbon Nanotubes of 1-nm Diameter", *Nature* **363**, 603-605, 1993.
6. D. S. Bethune, C. H. Kiang, M. S. de Vries, G. Gorman, R. Savoy, J. Vazquez and R. Beyers, "Cobalt-Catalyzed Growth of Carbon Nanotubes with Single-Atomic-Layerwalls", *Nature* **363**, 605-607, 1993.
7. L. S. Schadler, S. C. Giannaris and P. M. Ajayan, "Load Transfer in Carbon Nanotube Epoxy Composites", *Appl. Phys. Lett.*, **73**, 3842-3844, 1998.
8. A. A. Mamedov, N. A. Kotov, M. Prato, D. M. Guldi, J. P. Wicksted and A. Hirsch, "Molecular Design of Strong Single-Wall Carbon Nanotubes/Polyelectrolyte Multilayer Composites", *Nature Mater.*, **1**, 190-194, 2002.
9. G. -D. Zhan, J. D. Kuntz, J. Wan and A. K. Mukherjee, "Single-Wall Carbon Nanotubes as Attractive Toughening Agents in Alumina-based Nnaocomposites", *Nature Mater.*, **2**, 38-42, 2003.
10. X. Wang, N. P. Pature and H. Tanaka, "Contact-Damage-Resistant Ceramic/Single-Wall Carbon Nanotubes and Ceramic/Graphite Composites", *Nature Mater.*, **3**, 539-544, 2004.

11. R. Andrews, D. Jacques, A. M. Rao, T. Rantell, F. Derbyshire, Y. Chen, J. Chen and R. C. Haddon, "Nanotube Composite Carbon Fibers", *Appl. Phys. Lett.*, **75**, 1329-1331, 1999.
12. B. Vigolo, A. Pénicaud, C. Coulon, C. Sauder, R. Pailler, C. Journet, P. Bernier and P. Poulin, "Macroscopic Fibers and Ribbons of Oriented Carbon Nanotubes", *Science* **290**, 1331-1334, 2000.
13. H. W. Zhu, C. L. Xu, D. H. Wu, B. Q. Wei, R. Vajtai, P. M. Ajayan, "Direct Synthesis of Long Single-Walled Carbon Nanotubes Strands", *Science* **296**, 884-886, 2002.
14. A. B. Dalton, S. Collins, E. Muñoz, J. M. Razal, V. H. Ebron, J. P. Ferraris, J. N. Coleman, B. G. Kim and R. H. Baughman, "Super-Tough Carbon-Nanotube fibres", *Nature* **423**, 703 (2003).
15. Y. -Li. Li, I. A. Kinloch and A. H. Windle, "Direct Spinning of Carbon Nanotubes Fibers from Chemical Vapor Deposition Synthesis", *Science* **304**, 276-278, 2004.
16. L. M. Ericson, H. Fan, H. Peng, V. A. Davis, W. Zhou, J. Sulpizio, Y. Wang, R. Booker, J. Vavro, C. Guthy, A. N. G. Parra-Vasquez, M. J. Kim, S. Ramesh, R. K. Saini, C. Kittrell, G. Lavin, H. Schmidt, W. W. Adams, W. E. Billups, M. Pasquali, W. -F. Hwang, R. H. Hauge, J. E. Fischer and R. E. Smalley, "Macroscopic, Neat, Single-Walled Carbon Nanotubes Fibers", *Science* **305**, 1447-1450, 2004.
17. M. -F. Yu, B. S. Files, S. Arepalli and R. S. Ruoff, "Tensile Loading of Ropes of Single Wall Carbon Nanotubes and their Mechanical Properties", *Phys. Rev. Lett.*, **84**, 5552-5555, 2000.
18. M. Omori, "Sintering, Consolidation, Reaction and Crystal Growth by the Spark Plasma System (SPS)", *Mater. Sci. Eng. A*, **287**, 183-188, 2000.
19. M. Omori, A. Okubo, M. Otsubo, T. Hashida and K. Tohji, "Consolidation of Multi-Walled Carbon Nanotube and Hydroxyapatite Coating by the Spark Plasma System (SPS)", *Key Eng. Mater.*, **254-256**, 395398, 2004.
20. H. Matsuno, A. Yokoyama, F. Watari, M. Uo and T. Kawasaki, "Biocompatibility and Osteogenesis of refractory metal implants, titanium, hafnium, niobium, tantalum and rhenium", *Biomaterials*, **22**, 1253-1262, 2001.
21. A. Yokoyama, H. Matsuno, S. Yamamoto, T. Kawasaki, "Tissue Response to A Newly Developed Calcium Phosphate Cement Containing Succinic Acid and Carboxymethyl-Chitin", *J. Biomed. Mater. Res.*, **64A**, 491-501, 2003.

*hige@bucky1.kankyo.tohoku.ac.jp; phone +81 22 217 7392; fax +81 22 217 7392

Application of multi-walled carbon nanotubes to CdS photocatalytic system

Y.SAWADA¹, T.ARAI², Y.SATO¹, K.SHINODA¹, B.JEYADEVAN¹, K.TOHJI¹

¹Graduate School of Environmental Studies, Tohoku University, Sendai, Japan

²Institute of Fluid Science, Tohoku University, Sendai, Japan

ABSTRACT – Cadmium Sulfide (CdS) semiconductor particles that operate as a photocatalyst in the visible light region were deposited on the surface of modified multi-walled carbon nanotubes (MWCNTs) by chemical bath deposition (CBD) method. The enhancement of photocatalytic activity of CdS/MWCNTs was observed in the hydrogen generation experiment carried out using the visible light radiation and role of MWCNTs as an electrode was confirmed. Modifying the surfaces of MWCNTs with induced defects controlled the particle CdS size. The increase of specific surface area of CdS resulted in decreased amounts of hydrogen generated. Consequently, the photocatalytic activity of CdS/MWCNTs was strongly influenced by the state of the surface and electronic properties of MWCNTs.

1. INTRODUCTION

Recently, there has been considerable interest in hydrogen energy, which is believed to be the answer for the environmental problem faced by the mankind at present. From this point of view, the photocatalytic system that produces hydrogen with solar energy has been considered very promising. We have been successful in effectively splitting hydrogen sulfide molecule using Pt supported CdS photocatalyst with a specific morphology (stratified structure) in the visible light region^[1]. Though the physical structure of the particle was very vital for the separation of the oxidation-reduction reaction sites, the photocatalytic efficiency of these particles strongly depended on Pt that acts as an electrode. As Pt is very costly, alternative material has to be considered for practical application.

Since the discovery of carbon nanotubes with unique properties in 1991^[2], they have been considered for many applications. We believe that carbon nanotubes could be used as CdS photocatalyst support because of their size, chemical stability, and semiconductor properties. The deposition of CdS on MWCNTs may promote the formation of small particles and prevent particle aggregation. Additionally, we desire to achieve the separation of oxidation-reduction reaction sites using the tubular structure and electric properties of the nanotubes.

In this paper, we report the effect of the surface of MWCNTs on their electronic state, and photoreactivity of CdS/MWCNTs.

2. EXPERIMENT

2.1 Preparation of surface modified MWCNTs

MWCNTs were synthesized by chemical vapor decomposition method using metal catalysts (NanoLab Inc.). The as-grown samples were air-oxidated and acid treated to remove the metal

catalysts. Then, these samples were treated to obtain MWCNTs with different surface properties for the deposition of CdS. Here, we prepared four types of samples for this study. First, the purified sample was treated with ozone to make the surface of the nanotubes have hydrophilic nature. Here, 100 mg of MWCNTs were dispersed in 300 ml of toluene using ultrasonication. Then, the suspension was bubbled with ozone gas for one hour. The ozonized sample was filtered and washed out with ethanol. This sample is named as 'sample A'. Then, the sample B was prepared by annealing the purified nanotubes at 2273 K for 5 hours in high vacuum furnace and treated with ozone. The annealing treatment improved the crystallinity of the MWCNTs surface through the rearrangement of carbon atoms by thermal energy. And the ozone treatment was carried out to make the nanotube surface hydrophilic. Then, samples C and D were prepared from cut purified nanotubes. In the case of sample C, 100 mg of purified MWCNTs was added into 100 ml of mixed acid (conc.H₂SO₄ (95%): conc.NO₃ (60%) = 75 ml : 25 ml) solution and ultrasonicated and stirred for 3 hours. This process facilitates the cutting and surface modification in a single step^{[3][4]}. Then, the cut sample was annealed and ozonated under conditions stipulated in the preparation of sample B to obtain sample D.

All the samples were characterized by Raman spectroscopy (Jobin Yvon Spex; T64000), scanning electron microscope (SEM, Hitachi; 4100) and transmission electron microscope (TEM, Hitachi; HF-2000).

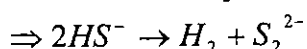
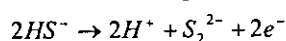
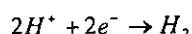
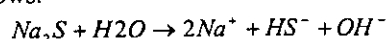
2.2 CdS deposition on MWCNTs

CdS was deposited by CBD method on MWCNTs samples (A)-(D). The deposition of CdS particles on MWCNTs were realized by introducing specified amount of MWCNTs into 100 ml of 0.01M 3CdSO₄ · 8H₂O, 1.0M NH₃, and 0.01M SC(NH₂)₂ mixed solution and heating to

358 K and allowed to cool down to room temperature in one hour. The reaction conditions, such as reaction time, temperature, and concentration of reagents were kept constant, but the amount of MWCNTs introduced was adjusted to maintain the surface area of the sample equal. CdS/MWCNTs were analyzed by SEM, TEM, and XRD.

2.3 Irradiation Experiment

Photocatalytic reactivities of the CdS/MWCNTs samples were evaluated by splitting the hydrogen sulfide molecule using the visible light irradiation. A specified amount of CdS/MWCNTs samples were introduced into 0.1M Na₂S solution. The hydrogen generation reaction from Na₂S solution was assumed to occur as follows:



Solar spectrum was simulated using Xenon Lamp (Wakomu-Denso: KXL-552HPF: 550W). The amount of hydrogen generated in 4 hours was recorded.

3. RESULT AND DISCUSSION

3.1 Preparation of MWCNTs

As shown in Fig.1, the MWCNTs were free of impurities and confirmed the effectiveness of the purification process. Then, the ozonized purified MWCNTs were dispersed well in distilled water

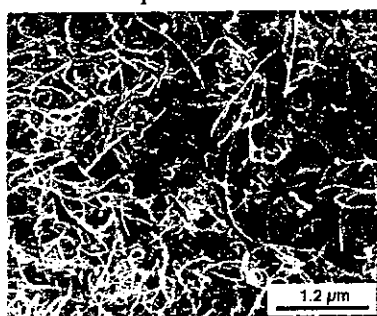


Fig1. SEM image of purified MWCNTs

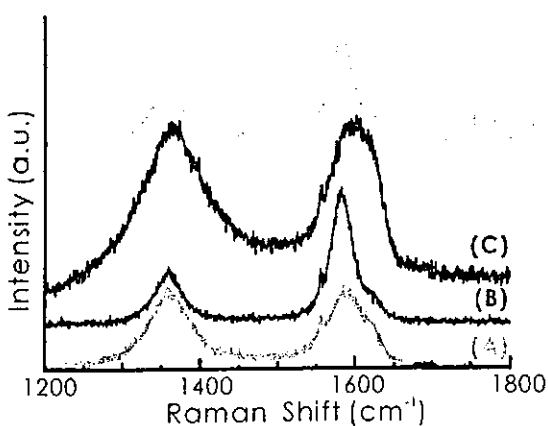


Fig.2 Raman spectra of four samples (A)-(D).

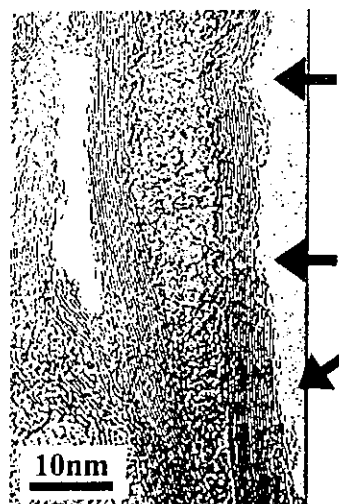


Fig.3 TEM image of cut MWCNTs (defects are indicated by arrows)

suggesting that the surface of the nanotubes has become hydrophilic. The hydrophilic nature of the surface is believed due to the presence of oxidized functional groups. The Raman spectrum of MWCNTs (Fig.2) showed the two main peaks centered at 1580 cm⁻¹ and 1350 cm⁻¹ derived from crystalline graphite (G-band) and defects or disordered crystalline graphite (D-band) respectively. We can discuss the crystallinity of MWCNTs by comparing the G and D band ratio (G/D). As shown in Fig.2, we observed the improvement of the same by annealing the samples at 2273 K for 5 hours in vacuum. The TEM micrograph of the cut sample is shown in Fig.3. The surface roughness observed in Fig.3 was due to the defects created by the acid treatment. Cut nanotubes also exhibited affinity towards water as in the case of sample A. Table.1 shows the results of specific surface area of each sample measure by using the BET method. Though the specific surface area of oxidized MWCNTs is expected to increase^{[5][6]}, the cut and ozone treated samples showed a decrease in surface area. Presumably, strong oxidizing power of the mixed acid solution and ozone may have converted the graphite sheets into amorphous carbon. Furthermore, the specific surface area of annealed samples decreased significantly. This is believed due to clean, defect-free smoothed surfaces of the nanotubes.

	Purified MWCNTs	(A)	(B)	(C)	(D)
Specific Surface area (m ² g ⁻¹)	246.6	241.2	146.3	209.3	155.9

Table1. Measuring results of specific Surface area

3.2 Properties of CdS/MWCNTs

From the XRD patterns of the CdS/MWCNTs (Fig.4), the presence of cadmium compounds were identified and found to be that of cubic CdS and hexagonal cadmium hydroxide (Cd(OH)₂). As seen from the TEM photographs in Fig. 5, the particle sizes of the CdS deposited on the nanotubes differ. The UV-VIS spectra of the

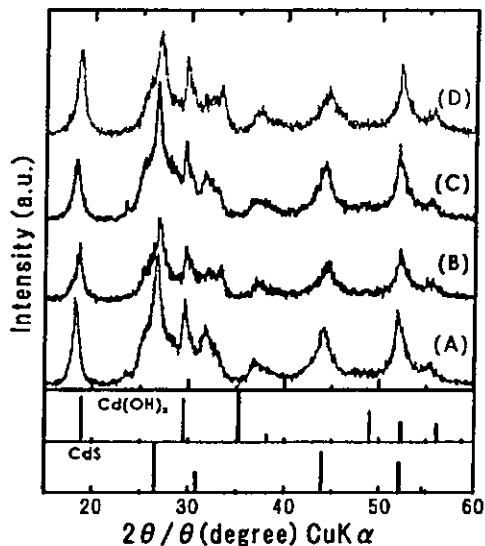


Fig.4 XRD patterns of CdS/MWCNTs

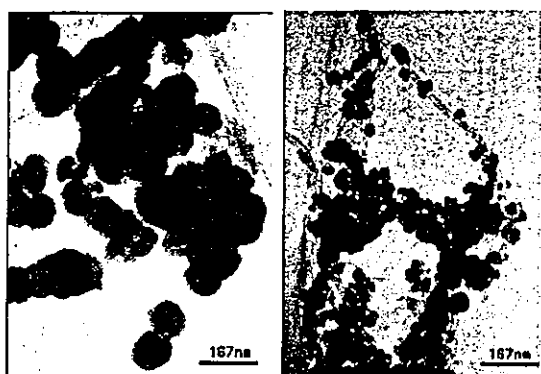


Fig.5 TEM images of CdS/MWCNTs left;(B), right;(C)

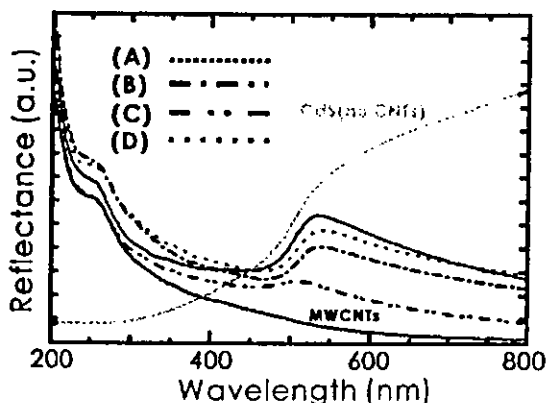


Fig.6 UV-VIS spectra of CdS/MWCNTs samples (A)-(D) are shown in Fig. 6. Though the absorption edge of all the samples appeared around 500 nm, the reflection coefficients of the samples varied. This may be due to the variation in particle morphology. In the case of CdS deposited on a rough glass surface by CBD method, the particle size becomes smaller^[7]. If we compare the nanotube surfaces, sample B and C has smooth and rough textures respectively. And also, the size of the particles deposited on sample B and C were large and small respectively. This was in agreement with what was observed in the case of CdS deposited on rough glass surface. It is inferred that the difference in particle size is due

to the difference in free energy change during nucleation caused by the surface morphology of the nanotubes.

3.3 Photoreactivity of CdS/MWCNTs

Fig.7 shows the results of hydrogen generation experiment carried out using the CdS/MWCNTs photocatalyst dispersed in Na₂S solution and exposed to visible light irradiation. The results include that of CdS without MWCNTs as a control. It was obvious that the use of MWCNTs as a substrate had an effect on the photocatalytic activities of CdS. Among the samples tested, highest activity was reported for the sample B. The poor activities of other samples were considered due to the difference in the crystallinity of the MWCNTs. In the case of sample A, the surface was not free of defects. On the other hand, in the case of sample C, the surface was full of defects. Though the sample D was annealed to reduce the number of defects on the surface, the photoactivity was not enhanced enough compared with sample B. However, activity of sample D was higher than that of C and almost equal to A. Considering the above facts, we believe that the photocatalytic activity is closely related to the crystallinity of the MWCNTs. The reason being that the electronic property of the MWCNTs depends very much on the crystallinity^[8]. Thus the electron transport property (which is the key issue in photocatalysis) have been enhanced in highly crystalline MWCNTs. MWCNTs supposed to play a role similar to that of platinum on platinum supported CdS and also helps to separate the oxidation-reduction reaction sites for promoting photocatalytic activities by preventing recombination of photo excited electrons and holes.

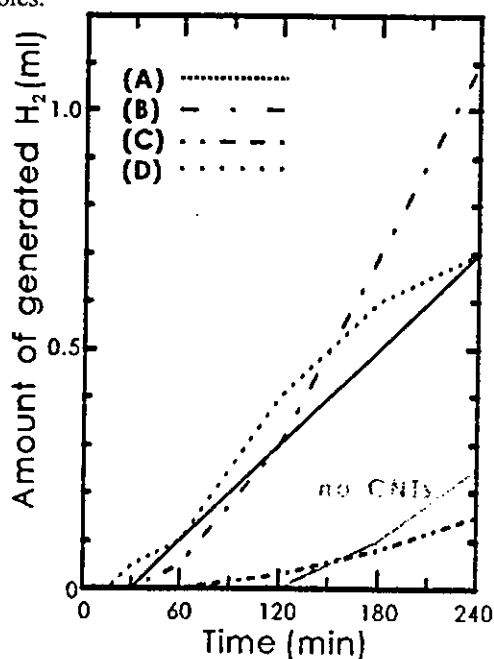


Fig.7 Amount of generated hydrogen

4. CONCLUSION

CdS was deposited on the surface modified MWCNTs by CBD method. The deposited particle sizes become smaller with increasing defects. The results of hydrogen generation experiment suggested that photocatalytic activities were dependent on the crystallinity of MWCNTs rather than CdS particle size. As the electric property is linked to the crystallinity of the nanotubes, it is assumed that photo excited electrons are easily transferred from CdS to MWCNTs and moved to reaction sites. In other words, it is predicted that the MWCNTs act as a metal catalyst such as Pt that causes site separation effect.

5. REFERENCE

- [1]T.Arai, S.Sakima, Y.Sato, K.Shinoda, B.Jeyadevan and K.Tohji
Shigen-to-Sozai, **119**, 713-720 (2003)
- [2]S.Iijima, *Nature*, **354**, 56 (1991)
- [3]S.F.McKay, *J.Appl.Phys.*, 1964, **35**, (1992)
- [4]J.Liu *et al.*, *Science*, 1253,**280**,(1998)
- [5]Yan-Hui.Li, Shuguang.Wang, Zhaokun Luan, Jun Ding, Cailu Xu and Dhai Wu,
Carbon, **41**, 1057-1062 (2003)
- [6]A.M.Zhang, J.L.Dong, Q.H.Xu, H.K.Rhee and X.L.Li,
Catalysis Today, **93-95**, 347-352 (2004)
- [7]T.Yakubo, Master's thesis (2002)
- [8]J.C.Charlier, *Acc. Chem. Res.* , **35**, 1063-1069 (2002)

Consolidation of Multi-Walled Carbon Nanotube and Hydroxyapatite Coating by the Spark Plasma System (SPS)

M. Omori¹, A. Okubo¹, M. Otsubo², T. Hashida² and K. Tohji²

¹ Institute for Materials Research, Tohoku University, 2-1-1 Katahira, Aoba-ku, Sendai 980-8577, Japan, email: mamori@imr.tohoku.ac.jp

² Graduate School of Engineering, Tohoku University, Aoba, Aramaki, Aoba-ku, Sendai, 980-8577, Japan

Keywords: carbon nanotube, multi-walled carbon nanotube, consolidation of carbon nanotube, spark plasma system (SPS), spark plasma sintering (SPS), hydroxyapatite coating

Abstract. A multi-walled carbon nanotube (MWNT) was mixed with phenol resin and consolidated by the spark plasma system (SPS). Properties of the MWNT consolidated at 1200°C at 120 MPa were as follows: bulk density was 1.74 g/cm³; apparent porosity was 16.3%; Young's modulus was 11.1 GPa. Hydroxyapatite was coated on the consolidated MWNT at 1000°C and 120 MPa by SPS, using the suspension prepared from 6 moles of CaHPO₄·2H₂O and 4 moles of Ca(OH)₂.

Introduction

Carbon nanotubes (CNT) consist of single-walled carbon nanotubes (SWNT) and multi-walled carbon nanotubes (MWNT) and have been attracting a lot of attention since their discovery [1]. It is said that molecular circuit devices will be fabricated from SWNT [2]. MWNTs are composed of various kinds of tube diameters and a number of carbon network layers. CNT are still expensive, but the cost of their fabrication will surely decrease in the near future. Low-cost CNTs will be used for fillers of composites and starting materials to produce structural and/or functional compacts. Graphite is a hard-to-sinter material, and its powder can only be sintered at very high temperatures under pressing [3]. The sintering ability of CNT is the same as that of graphite, and advanced techniques are needed to consolidate it at lower temperatures, before the transformation into graphite. The spark plasma system (SPS) has been developed for sintering of metal and ceramics in the plasma and electric field [4, 5], and it is used for consolidation of various kinds of materials such as metals, ceramics and polymers [6]. The bioactivity of graphite is not excellent. The best way to increase the bioactivity of the consolidated MWNT is deposition of hydroxyapatite (HA) films on it. Plasma spraying is widely used for manufacturing HA coating on Ti or Co-Cr-based implants. However, a multitude of phase changes occurs at high temperatures of the plasma spraying process [7]. Two compounds of 6 moles of CaHPO₄·2H₂O and 4 moles of Ca(OH)₂ reacted at 150°C to produce HA and H₂O by the hydrothermal hot-pressing method [8]. This reaction is able to apply to HA coating on biomaterials because the reaction product is only HA except for H₂O.

In this paper, the MWNT was mixed with phenol resin in ethanol. After removing the ethanol and decomposing the phenol resin by heating, the mixture of the MWNT and the amorphous carbon was consolidated by SPS. The consolidated MWNT was dipped in the suspension of 6 moles of CaHPO₄·2H₂O and 4 moles of Ca(OH)₂. The two compounds reacted and bonded to the consolidated MWNT at 1000°C at 120 MPa by SPS.

Experimental procedures

Consolidation of MWNT

CNT used for the consolidation was MWNT (NanoLab Inc., USA, 80% purity). The MWNT was purified to remove a metal catalyst using a solution of 50% HNO₃. Phenol resin was dissolved in ethanol. The MWNTs were put in the ethanol solution. After evaporating ethanol, the phenol resin film on the MWNT was decomposed at about 200°C in air. The coated MWNTs were put in a graphite die and set in the spark plasma system (SPS) (Sumitomo Coal Mining, Japan, SPS-1050). The consolidation was carried out between 1000°C and 1600°C at 120 MPa in a vacuum. In case of the consolidation at 1000°C, the consolidation temperature was raised as follows: heating rate from 0°C to 900°C at 100°C/min, from 900°C to 980°C at 20°C/min, from 980°C to 1000°C at 5°C/min and holding time at 1000°C for 5 min.

The microstructure of the consolidated MWNT was analyzed by a transmission electron

microscope (JEOL, Japan, JT-007). The polished surface of the consolidated MWNT was observed with an optical microscope (Nikon, Japan, N-01). X-ray diffraction (XRD) was carried out on the MWNT and the consolidated one using Cu K α line by an X-ray diffractometer (Rigaku, Japan, Rotaflex, RU-200B). Density of the consolidated disk was determined based on Archimedes' principle using water. Elastic modulus of disk samples (3 mm in thickness and 20 mm in diameter) was measured by a pulse-echo overlap ultrasonic technique, using an ultrasonic detector (Hitachi Kenki Co. Ltd., Japan, ATS-100) and a storage oscilloscope (Iwasaki Tsushinki Co. Ltd., Japan, DS6411).

Coating of HA on the consolidated MWNT

CaHPO $_4$ ·2H $_2$ O (6 moles) and Ca(OH) $_2$ (4 moles) powders (Wako Pure Chemical Ind., Japan, reagent grade) were used to form HA films. These powders were suspended in distilled water using glycolic acid (Wako Pure Chemical Ind., Japan, reagent grade). The consolidated MWNT (1 x 1 x 5 mm 3) was dipped in the suspension and dried. The coated MWNT was put in the graphite die with carbon powders and set in SPS. The coating of HA was carried out at 1000°C at 120 MPa in a vacuum. The heating rate was controlled as follows: from 20°C to 900°C at 100°C/min, from 900°C to 980°C at 20°C/min and from 980°C to 1000°C at 5°C/min. The holding time at 1000°C was 5 min.

Results and discussion

Consolidation of MWNT

An X-ray diffraction pattern of the MWNT was similar to that of graphite (small squares in Fig. 1). As shown in the transmission electron micrograph (TEM) of Fig. 2, the MWNT consisted of varied tube diameters. The dispersion of the diameter was mainly from 10 nm to 50 nm, and a thick MWNT of 200 nm in diameter was found among them.

The MWNT had about 20% amorphous carbon and was not consolidated by SPS. This amorphous carbon did not enhance the consolidation of the MWNT by SPS. A phenol resin was added to achieve the consolidation, and its carbon residue was of about 20%. The optical micrograph revealed that the MWNT consolidated with the 30% phenol resin contained coarse pores. There were no coarse pores in the MWNT consolidated with 50% phenol resin. It was considered that the addition of the 50% phenol resin was adequate to obtain the dense compact. The X-ray diffraction pattern of the MWNT consolidated at 1000°C was similar to those of the MWNT and graphite.

When the consolidation was carried out at 1200°C and at 1400°C, the (101) peak was strong compared with other ones. The pattern of the MWNT consolidated at 1400°C was slightly different from that of the MWNT and graphite. The difference was emphasized on the pattern of the MWNT consolidated at 1600°C, but the intensity of the (101) peak decreased, as shown in Fig. 1. The new diffraction peaks did not correspond to those of graphite. Fig. 3 shows the TEM image of the MWNT consolidated at 1600°C with 30% phenol resin. The MWNT was partly decomposed and converted into different

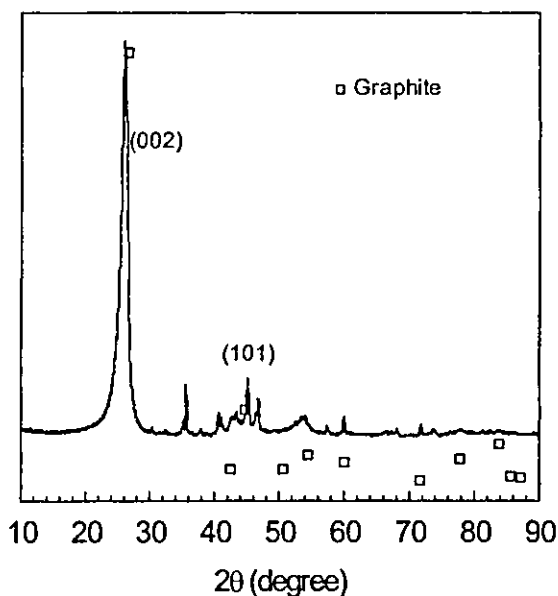


Fig. 1 XRD pattern of the MWNT consolidated at 1600°C.

Table 1 Density and mechanical properties of the consolidated MWNT

Consolidation temperature (°C)	Bulk density (g/cm 3)	Apparent porosity (%)	Closed porosity (%)	Young's modulus (GPa)	Poisson's ratio
1000	1.67	16.7	9.6	3.05	-0.62
1200	1.74	16.8	6.4	11.1	0.074
1400	1.73	15.6	8.1	10.1	0.034

compounds from graphite. MWNT is not decomposed until 2400°C by heating [9]. The SPS process consists of some effects such as the spark plasma, electric field and others, and carbon fibers are decomposed into powders by the SPS treatment [6]. The carbon network of the MWNT should be partly decomposed by the spark plasma and resulted in new structures different from graphite.

The density and mechanical properties are shown in Table 1. The low bulk density of the MWNT consolidated at 1000°C indicated that the consolidation was not accomplished. The bulk density of 1.74 g/cm³ was not high and depended on the tube structure because there were no coarse pores. The apparent porosity was almost the same for all consolidated MWNT. The closed porosity was calculated from the apparent porosity and theoretical density of graphite (2.266 g/cm³). Since the theoretical density of the MWNT must be lower than that of graphite, the closed porosity should decrease less than the values indicated in Table 1. Young's modulus and Poisson's ratio were measured on the surface where the MWNT was aligned parallel to the pressing direction of SPS. Young's modulus of the MWNT consolidated at 1000°C was lower than that of the ones consolidated

1200°C and 1400°C. The Young's modulus of 11.1 GPa of the consolidated MWNT was not low, considering the density of the consolidated MWNT and that of 16 GPa of a commercial graphite product with high density of 2.0 g/cm³. Given that, the Young's modulus of human bone is 7 - 30 GPa [9], the consolidation of the MWNT could produce the material with the low modulus. Poisson's ration was negative for the MWNT consolidated at 1000°C, and was very little for the ones consolidated at 1200°C and 1400°C. The negative Poisson's ratio indicated that the bond between the MWNTs was not completed at 1000°C, which is consistent with the Young's modulus of 3.05 GPa.

The bending strength of the consolidated MWNT was measured by a three-point bending test method, but it was not obtained. The sample for the bending test was curved by stress at first, and then it was fractured. Bending strength of ductile materials like metals cannot be measured. The consolidated MWNT behaved in the same way as metal for bending test. Bending strength of human bone is 50 - 150 MPa [9], and that of the consolidated MWNT seemed to be lower than it. It is obvious the strength of the consolidated MWNT is not enough for application to human bone at the moment.

Coating of HA on the consolidated MWNT

CaHPO₄·2H₂O and Ca(OH)₂ were easily suspended in water compared with HA powder because they contained an OH group or H₂O. The mirror surface of the consolidated MWNT was inadequate for HA coating. A coarse surface was prepared by polishing with SiC powders of 64 μm. Two suspended compounds of 6 moles of CaHPO₄·2H₂O and 4 moles of Ca(OH)₂ were coated on the consolidated MWNT and reacted at 1000°C and 120 MPa by SPS. The reacted film was identified as HA by X-ray diffractometry. Fig. 4 shows an optical micrograph of the consolidated MWNT coated with HA. The HA film did not contain cracks. The coated HA seemed bonded with the rough surface of the consolidated MWNT, although the bonding strength was not determined. The bonding was partly based on the anchor effect of the coarse surface. It was not clear whether



Fig. 2 TEM image of MWNT.

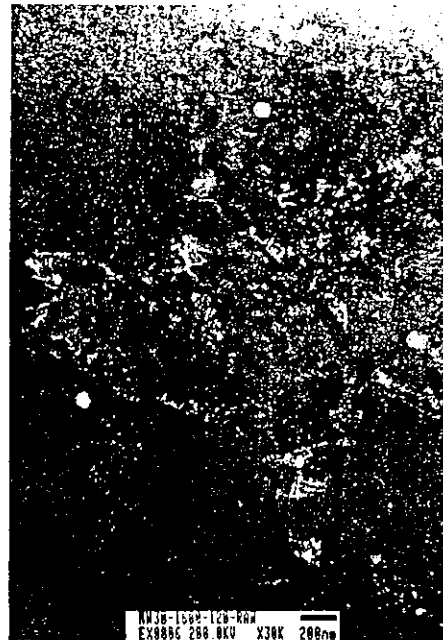


Fig. 3 TEM image of the MWNT consolidated at 1600 °C.

the chemical bond was associated with the bonding. The compounds of 6 moles of $\text{CaHPO}_4 \cdot 2\text{H}_2\text{O}$ and 4 moles of $\text{Ca}(\text{OH})_2$ were allowed to dehydrate and produce HA at high pressure, such as 120 MPa. HA was not formed at 1000°C and 10 MPa from those compounds by SPS. The reaction temperature decreased from 1000°C to 600°C with increasing the pressure from 120 MPa to 300 MPa [13], but the film coated at the low temperature peeled. HA can be formed from CaHPO_4 or $\text{CaHPO}_4 \cdot 2\text{H}_2\text{O}$ at 200°C by hydrothermal technique [10-12]. The reaction temperature by SPS was higher than those of hydrothermal and hydrothermal hot-pressing methods. The hydrothermal reaction requires water to complete the formation of HA, but SPS does not.

Conclusions

The MWNT containing about 20% of amorphous carbon was not consolidated by SPS. Amorphous carbon transformed from the phenol resin enhanced the consolidation. The structure of the consolidated MWNT was almost the same as that of graphite. The MWNT in the consolidated form was aligned in the direction parallel to the (101) plane of graphite. The consolidated MWNT was decomposed at temperatures higher than 1400°C. Properties of the MWNT consolidated at 1200°C and 120 MPa were as follows: density was 1.74 g/cm³; apparent porosity was 16.8%; Young's modulus was 11.1 GPa; Poisson's ratio was 0.074.

HA was coated on the consolidated MWNT at 1000°C at 120 MPa, using the suspension prepared from 6 moles of $\text{CaHPO}_4 \cdot 2\text{H}_2\text{O}$ and 4 moles of $\text{Ca}(\text{OH})_2$. HA was not cracked and tightly covered the surface of the consolidated MWNT.

Acknowledgments

This study is supported by Research on Advanced Medical Technology in Health and Labour Sciences Research Grants from Ministry of Health, Labour and Welfare of Japan. The authors are thankful to Yoshihiro Murakami, Shun Ito, Yuichiro Hayasaka and Yoshiyuki Sato for the measurements of X-ray diffraction patterns and observations of transmission electron microscope and optical microscope.

References

- [1] S. Iijima: *Nature*, Vol. 354 (1991), p. 56.
- [2] L. Chico, L. X. Menedic, S. G. Louie and M. L. Cohen: *Phys. Rev.*, B54 (1996), p. 2600.
- [3] H. Boeder and E. Fitzer: *Carbon*, Vol. 8 (1970), p. 453.
- [4] K. Inoue: US Patent, No. 3,241,956 (1966).
- [5] K. Inoue: US Patent, No. 3,250,892.
- [6] M. Omori: *Mater. Sci. Eng.*, A287 (2000), p. 183.
- [7] S. R. Radin and P. Ducheyne: *J. Mater. Sci.: Mater. Med.* Vol. 3 (1992), p. 33.
- [8] K. Hosoi, T. Hashida, H. Takahashi, N. Yamazaki and T. Korenaga: *J. Am. Ceram. Soc.*, Vol. 79 (1996), p. 2771.
- [9] A. Bougrine, N. Dupont-Pavlovsky, A. Naji, J. Ghanbaja, J. F. Mareche and D. Billaud: *Carbon*, Vol. 39 (2001), p. 685.
- [10] L. H. Hench: *J. Am. Ceram. Soc.*, Vol. 81 (1998), p. 1705.
- [11] A. P. Peroff and A. S. Posner: *Science*, Vol. 124 (1958), p. 583.
- [12] E. Hayek, W. Boehler, J. Lechleitner and H. Petter: *Z. Anorg. Allg. Chem.*, Vol. 295 (1958), p. 241.
- [13] M. Omori, T. Onoki and T. Hashida: Unpublished data

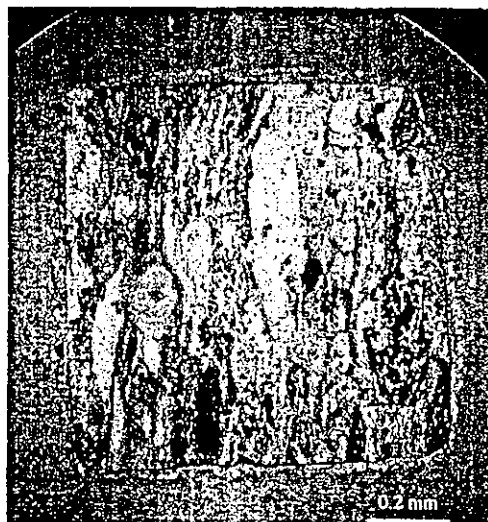


Fig. 4 Optical micrograph of the consolidated MWNT coated with HA.

研 究

Preparation of Multi-Walled Carbon Nanotube Compact by the Spark Plasma System (SPS)

Mamoru Omori^{★1}, Akira Okubo^{★2}, Toshiyuki Hashida^{★1} and Kazuyuki Tohji^{★1}^{★1}Graduate School of Engineering, Tohoku University, 6-6-01 Aoba, Aramaki, Aoba-ku, Sendai 980-8579.^{★2}Institute for Materials Research, Tohoku University, 2-1-1 Katahira, Aoba-ku, Sendai 980-8577.

Received September 30, 2004

SYNOPSIS

The multi-walled carbon nanotube (MWNT) was not consolidated without additives by the spark plasma system (SPS). The phenol resin of 33 wt% was added to promote the consolidation. The MWNTs were aligned perpendicular to pressing direction of SPS in the consolidated compact. Bulk density and Young's modulus were more than 1.7 g/cm^3 and 10 GPa for the MWNT consolidated at 120 MPa at 1200 °C and 1400 °C. The fracture behavior on bending test was a kind of quasiplastic deformation and was based on pull out of the MWNTs.

KEY WORDS

Carbon nanotube, multi-walled carbon nanotube, consolidation of multi-walled carbon nanotube, multi-walled carbon nanotube compact

1 Introduction

Carbon nanotubes (CNTs), which were discovered in 1991¹⁾, are long, slender fullerenes where the walls of the tubes are hexagonal carbon (graphene layer) and often capped at each end. A lot of investigations have been shown that CNTs exhibit many superior mechanical, electric and electronic properties over any other known material and hold substantial promise as high-strength composites, energy storage and energy conversion devices, sensors, field emission displays and radiation sources, hydrogen storage media and nanometer-sized semiconductor devices²⁾. CNT consists of single-walled carbon nanotube (SWNT)^{3,4)}, double-walled carbon nanotube (DWNT)⁵⁾ and multi-walled carbon nanotube (MWNT)¹⁾. One of interests arises from their formidable mechanical properties, i.e. Young's modulus up to 640 GPa for SWNT⁶⁾ and up to 1800 GPa for MWNT⁷⁾ and strength up to 45 GPa for SWNT⁸⁾. CNT is expensive these days, but the cost of its fabrication will surely decrease in near future. Low-cost CNTs will be useful for fillers of composites and starting materials to produce structural and/or functional compacts. Graphite is a hard-to-sinter material, and its powder can only be sintered at very high temperatures under pressing⁹⁾. The sintering ability of CNT is the same as that of graphite, and advanced techniques are needed to consolidate it at lower temperatures before transforming into graphite. The spark plasma system (SPS) has been developed for sintering of

metal and ceramics in the plasma and electric field¹⁰⁾, and it has been used for consolidation of various kinds of materials such as metals, ceramics and polymers¹¹⁾.

In this paper, the MWNT was mixed with phenol resin in ethanol. After removing the ethanol and decomposing the phenol resin by heating, the mixture of the MWNT and the amorphous carbon transformed from the phenol resin was consolidated by SPS. Bulk density, Young's modulus, and Poisson's ratio were determined for the consolidated MWNT.

2 Experimental Procedures

CNT used for the consolidation was MWNT (NanoLab Inc., USA). Purity of the MWNT is more than 80%, and most of impurities are amorphous carbon. The MWNT was purified to remove metal catalysts by using 50% HNO₃ solution. The novolak type of phenol resin was dissolved in ethanol. The MWNTs were put in the ethanol solution. After evaporating ethanol, the phenol resin film on the MWNT was decomposed at about 200 °C in air. The coated MWNTs were put in a graphite die and set in the spark plasma system (SPS) (Sumitomo Coal Mining Co. Ltd., SPS-1050). The consolidation was carried out between 1000 °C and 1600 °C at 120 MPa in a vacuum. In case of the consolidation at 1000 °C, the consolidation temperature was raised as follows: heating rate from 0 °C to 900 °C at 100 °C/min, from 900 °C to 980 °C at 20 °C/min, from 980 °C

to 1000 °C at 5 °C/min and holding time at 1000 °C for 5 min.

The microstructure of the consolidated MWNT was analyzed by a transmission electron microscope (JEOL, JT-007). The polished surface of the consolidated MWNT was observed with an optical microscope (Nikon, N-01). X-ray diffraction (XRD) was carried out on the MWNT and the consolidated one using Cu K α line by an X-ray diffractometer (Rigaku, Rotaflex, RU-200B). Density of the consolidated disk was determined based on Archimedes' principle using water. Elastic modulus of disk samples (3 mm in thickness and 20 mm in diameter) was measured by a pulse-echo overlap ultrasonic technique, using an ultrasonic detector (Hitachi Kenki Co. Ltd., ATS-100) and a storage oscilloscope (Iwasaki Tsushinki Co. Ltd., DS6411).

3 Results and Discussion

The TEM image of the MWNT is shown in Fig. 1. The major part of tube diameters was 20–40 nm, and the biggest one rarely observed in the TEM photograph was about 200 nm. Amorphous carbon was identified by TEM and estimated less than 20 %.

The MWNTs consisting of amorphous carbon were not consolidated by SPS, which was not activated by SPS and did not play a roll to combine each MWNT. The phenol

resin was added to achieve the consolidation, and its carbon residue was of about 20%. The optical micrograph revealed that the MWNT consolidated with the 23% phenol resin contained coarse pores, as shown in Fig. 2. Much of the phenol resin promoted to get ride of the pores, and coarse pore was not produced in the MWNT consolidated with 33% phenol resin. Fig. 3 shows that there was no coarse pore on the polished surface of the consolidated MWNT. Block patterns were observed in these photographs and indicated a structural regularity. The MWNTs were very roughly aligned in the block, and direction of the alignment was different in each one. The reason why the MWNT was ordered by SPS was not clear, but the ordered alignment might be due to the weak interaction between MWNTs, SWNT forming the bundle structure by strong interaction.

TEM image of the MWNT consolidated at 1400 °C is shown in Fig. 4. The MWNTs were aligned in the plane perpendicular to the pressing direction of SPS. The same alignment was observed for the MWNT consolidated at 1000 °C and 1200 °C. The alignment was not random in



Fig.1 TEM image of MWNT.



Fig.2 Optical micrograph of the MWNT consolidated with 23 wt% of phenol resin at 1000 °C at 120 MPa for 5 min.

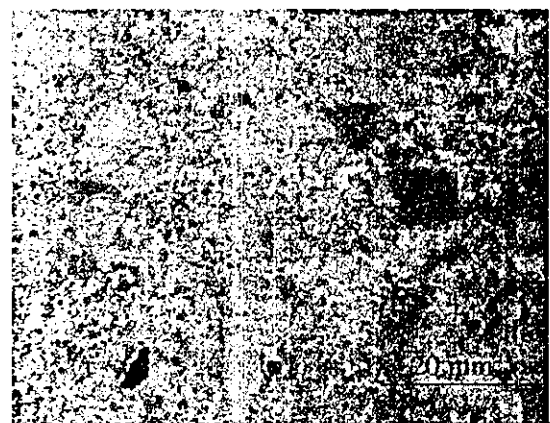


Fig.3 Optical micrograph of the MWNT consolidated with 33 wt% of phenol resin consolidated at 1200 °C at 120 MPa for 5 min.